

Full Length Research Paper

Preliminary dosimetric evaluation of a designed head and neck phantom for intensity modulated radiation therapy (IMRT)

K. M. Radaideh^{1*}, L. M. Matalqah^{2,3}, A. A. Tajuddin⁴, W. I. Fabian Lee⁵ and S. Bauk⁶

¹School of Physics, Universiti Sains Malaysia, 11800 Minden, Penang, Malaysia.

²School of Pharmaceutical Sciences, Universiti Sains Malaysia, 11800 Minden, Penang, Malaysia.

³School of Pharmacy, Alliance University College of Medical Sciences (AUCMS), 13200 Kepala Batas, Penang, Malaysia.

⁴Advanced Medical and Dental Institute, Universiti Sains Malaysia, 13200 Kepala Batas, Penang, Malaysia.

⁵Department of Radiotherapy and Oncology, Mount Miriam Cancer Hospital, Jalan Bulan, 11200 Penang Malaysia.

⁶Physics Section, School of Distance Education, Universiti Sains Malaysia, 11800 Minden, Penang, Malaysia.

Received 08 July, 2012; Accepted 16 November, 2012

The aims of this paper are to design, construct, and evaluate an anthropomorphic head and neck phantom for dosimetric verification of nasopharyngeal cancer treatment plan using intensity modulated radiation therapy (IMRT) technique. The phantom was designed as an assembly of thirty nine (39) transversal section slabs fabricated from Perspex material each with delineated planning target volumes (PTVs) and organ at risk (OARs) regions. Thermoluminescent dosimeter (TLD) was used after multiple calibration cycles. The phantom was imaged, planned, and irradiated by IMRT plan. The reproducibility of phantom measurements was checked by three identical IMRT irradiations. Four (4) nasopharyngeal patients' IMRT treatment plans were transferred to the phantom for dose verification. Phantom's measured doses were reproducible with less than 3.5% standard deviation. For the verification of IMRT patient's plans, the mean of percent dose differences between measured and calculated doses was found 6.2% (SD: 4.7) at OAR and 5.96% (SD: 2.5%) at PTV. The percentage dose deviation met the accuracy criteria of 7% at low dose regions. The standard deviation of TLD/TPS was 2.4% at PTV and 6.8% at OAR. This good agreement proves the feasibility of applying this phantom in IMRT dose verification.

Key words: Intensity modulated radiation therapy (IMRT) verification, head and neck phantom, thermoluminescent.

INTRODUCTION

Nasopharyngeal cancer is a challenging site for treatment with Intensity Modulated Radiation Therapy (IMRT) (Kam et al; 2003). Since IMRT treatments are complex in nature, significant inconsistencies between calculated

doses by Treatment Planning System (TPS) and those measured through *in-vivo* dosimetry, especially in the vicinity of critical structures, have been reported (Chung et al., 2005). TPS has many possibilities of dosimetric errors between planned and delivered treatments from the first step of the simulation process till the execution of treatment. The errors in TPS may arise from the use of inappropriate input dosimetric data in the treatment planning systems and improper modelling of rounded

*Corresponding author. E-mail: khaldoonmah1@yahoo.com.

multi-leaf collimator leaf ends (Cadman et al., 2002). Therefore, thorough quality assurance is required to minimize deviations between the planned radiation dose distribution and the dose that is actually delivered to the patient.

Quality assurance procedure is a practical method to verify the dose distributions with a sort of phantom in place of patients, by using radiation measuring devices as prerequisite for safe and efficient application. By exposing the phantom to a patient's set of beams, the treatment beams' true intensity distributions are measured against the intensity distributions and calculated in the TPS to determine if deviations are within the defined constraint levels. Other approaches have also been used to evaluate IMRT planning and delivery system combinations (Van Esch et al., 2002; Ezzell et al., 2003; Galvin et al., 2004; Gillis et al., 2005; Kinshikar et al., 2007). Molineu et al. (2005) designed an anthropomorphic phantom intended to evaluate an IMRT dose planning and delivery protocol. The phantom was designed as an outer plastic head-shaped shell filled with water. PTV was identified using polystyrene housing solid water and an acrylic was used for OAR.

Another head and neck phantom was designed for the purpose of IMRT treatments verification (Webster et al., 2008). The phantom was semi-anatomical Perspex with chamber insert to incorporate either a standard plotting tank chamber or a smaller pinpoint chamber. The validity of Perspex density assumption was checked by comparing the average density of the phantom, including oral cavity and esophageal heterogeneities, to the average density of seven (7) head-and-neck patients. The mean patient density was found to be 1.073 g.cm^{-3} (range: 1.018 to 1.236 g.cm^{-3}) as compared to $1.076 \pm 0.003 \text{ g.cm}^{-3}$ for the phantom (Webster et al., 2008).

An IMRT phantom (Scanditronix Wellhöver) is a commercially available phantom in the study center. This phantom includes 18 slabs with dimensions of $18 \times 18 \text{ cm}^2$ and 1 cm in thickness. This cubic phantom is a useful tool to measure doses at certain depth by dosimeters like TLDs and MOSFET, but unfortunately doses at a defined Organ at Risk (OAR) and planning target volume (PTV) regions cannot be predicted. As a consequence, anatomical head and neck phantom is mandatory in this study.

Nowadays, in most advanced centers, anthropomorphic phantoms are commonly used to evaluate the dose distribution. However, the medical physics community is still looking for a rather accurate, practical, cheap and easily available water substitute material to enhance precision and accuracy of radiotherapy dosimetry. Therefore, there is scope to design and fabricate comparable water substitute phantom materials for various dosimetric purposes with low cost and

easy availability. Phantom, made up of a material approximating soft tissue, is highly recommended by the American Association of Physics in Medicine, Radiation Therapy Committee (AAPM-RTC). It is needed to be used in assessing a patient's contour accurately and in verifying the IMRT techniques at both the commissioning and clinical stages. Ideally, these phantoms should be anatomical, with radiological properties identical to those of the soft tissues, and allow for a variety of measuring devices to be used in order to verify dose and distributions to a number of key positions throughout the target and normal-tissue volumes (ICRU Report 44, 1989). The availability of Perspex material is low cost and density similar to the average tissue and bone in the human head and neck region are considered when choosing Perspex as the material for fabricating this study's phantom (Webster et al., 2008).

The aims of this study were to design and fabricate a custom handmade head and neck phantom using Perspex material and to evaluate the fabricated phantom in a dosimetric verification of IMRT treatment dose planning and delivery to PTVs and OARs for nasopharyngeal cancer patients.

MATERIALS AND METHODS

TLDs annealing and calibration

Rod-shaped LiF:Mg,Ti (TLDs) (Bicron NE, USA) with dimensions of 0.1 cm (diameter) \times 0.6 cm (length), were used in this study. All TLD-100 were annealed using Nabertherm oven (Germany) by a thermal cycle: 1 h at 400°C , cooling for 2, 24 h at 80°C to associate the dipoles into trimmers, thus removing low temperature TL peaks and reducing fading when integrating intensity measurements (Horowitz, 1984; McKeever et al., 1995).

The TLDs were selected after a careful initialization procedure (Furetta and Weng, 1998).

For TLDs calibration, solid water phantom (Gammex RMI, Bad Munstereifel, Germany) and the calibrated ionization chamber, FC65-G (Wellhofer, Germany), were used to draw up the graph that shows the Percentage depth dose curve (PDD), and a correction factor can be obtained (Attix, 1986). As it was difficult to make holes within solid water phantom to place the TLDs, a number of 0.3 cm thickness Perspex slabs with dimensions of 30 cm (length) \times 30 cm (width) were fabricated. Holes with dimensions of 0.12 cm (depth) \times 0.12 cm (width) \times 0.6 cm (length) were drilled on the surface of the Perspex slabs for TLDs placement; all holes were drilled in a field size of $10 \times 10 \text{ cm}^2$ in the centre of the Perspex slabs. The slabs, which included rod TLDs, were slipped in-between the Gammex RMI solid water phantom at

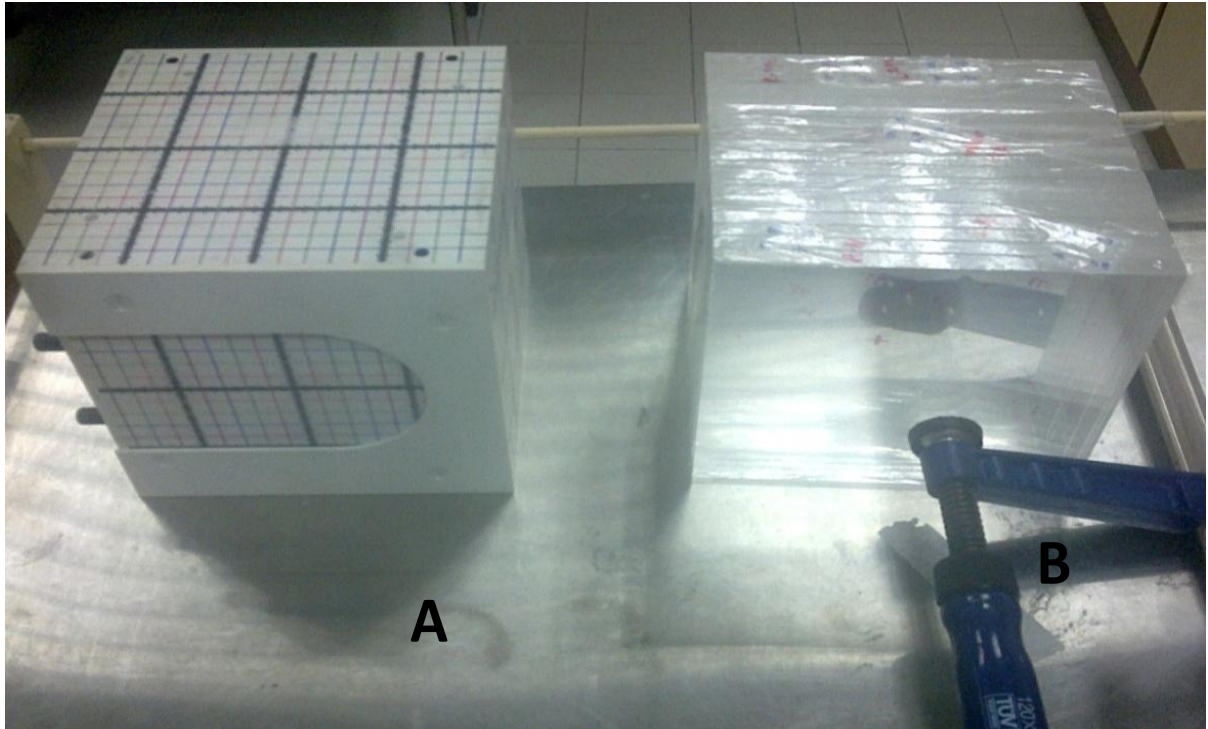


Figure 1. A: l'mRT phantom (Scanditronix Wellhöver), B: Fabricated cubic Perspex phantom.

d_{max} . A 6 MV photon beams from a Linear Accelerator (LINAC Siemens Artiste) was used to irradiate TLDs at a source-to-surface distance (SSD) of 100 cm with a ($10 \times 10 \text{ cm}^2$) field size. All TLDs' readings were performed by TLD reader Harshaw model 3500, USA.

As the accuracy of TLD measurements depend on the reproducibility of the results as measured by the standard deviation of each individual calibration factor, six (6) subsequent calibration cycles were carried out (McKeever et al., 1995; Furetta and Weng, 1998; Yazici, 2004; Radaideh and Alzoubi, 2010).

Percentage depth dose curve (PDD)

PDD curve study was performed by exposing the TLDs and ion chamber at different depths, ranging from 0 to 20 cm and 10 cm in thickness as full backscatter in the solid water and Perspex phantoms, at reference settings. The correction factor ($K_{\text{correction}}$) was obtained as a ratio of M_w and M_p , where M_w is the average of the five (5) ion chambers readings at 1.5 cm in a water phantom and M_p is the average of 10 TLD readings at the same depth in Perspex phantom. All readings of ion chamber were corrected for water temperature and atmospheric pressure.

Perspex validity test

A cubic Perspex phantom containing 18 slabs each with dimensions of 18 cm in length, 18 cm in width, and 1 cm in depth, similar to Scanditronix Wellhöver cubic phantom was designed (Figure 1). Matched reference points at both phantoms were determined.

The phantoms were lined up with lasers so that every point within the phantoms can be localized in three-dimensional space.

A CT scan was then performed for the cubic Perspex phantom to acquire the transverse images and locate the positions of the TLDs. These images were transferred to TPS (Oncentra Maherplan V3.3) computers, where the target volumes and normal tissues were outlined on the CT images, by then an IMRT treatment plan was developed for both phantoms. Both phantoms were planed using a nine-field IMRT treatment plan for nasopharyngeal cancer as follow: gross disease PTV 70 Gy and dose fractioned up to 33 for 5 days a week (Lee et al., 2009).

Thirty-seven (37) TLDs were placed at matched points within both phantoms and then exposed to three identical shots using a Siemens Artiste, set at 6 MV photons 100 Monitor Units (MU). After each individual shoot, TLDs were read and the average of the three (3) readings were



Figure 2. Anthropomorphic Perspex head and neck phantom after loading with TLDs.

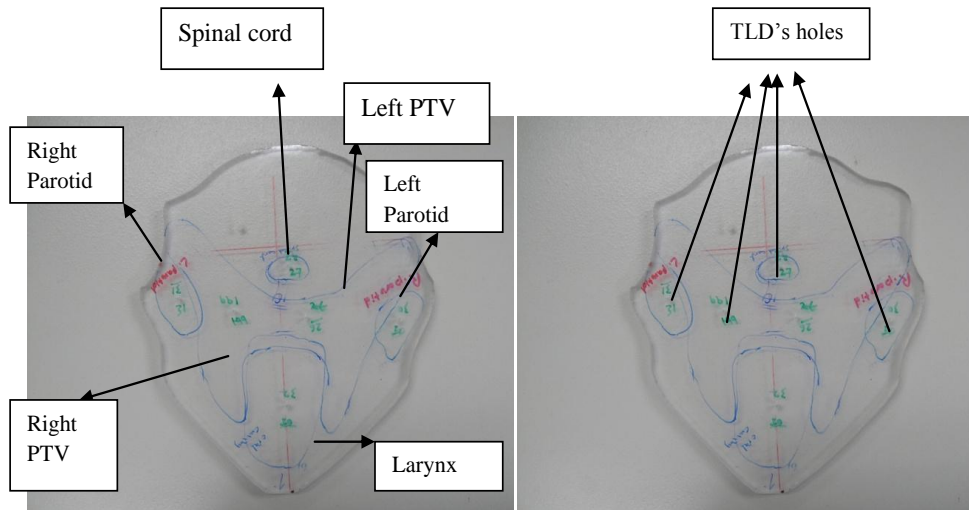


Figure 3. Perspex slabs with delineated Organs at Risk (OAR) and Planning Target Volume (PTV) boundaries. Abbreviations: TLD = Thermoluminescent Dosimeter; R= Right; L= Left.

considered and compared.

Phantom design and fabrication

In designing the phantom, attention was paid to the adequate representation of the dose distribution and standardization of the phantom's size and contouring (Figure 2). Computed tomography (CT) images for a number of nasopharyngeal patients using SIEMENS CT Scanner (SOMATOM Sensation Open, Germany) were obtained and transferred to TPS. With collaboration of a group of physicists and a radiotherapist and oncologist

practitioner, the dimensions of the head and neck regions were calculated using TPS and the average was considered, by then the primary and secondary PTVs and OARs were delineated and the print out of transverse sections were obtained.

By matching and contouring the images of the printed CT scan slices on Perspex boards, Thirty-nine slabs of Perspex were cut and when assembled they represented the model of a patient's head and neck regions (Figure 3). A Transparent 3M™ Polyethylene film tape, with 0.13 mm thickness (0.91 to 0.94 g.cm⁻³) and acrylic adhesive, was used to hold the slabs for phantom assembling.

Two perpendicular isocenter lines on the printed CT



Figure 4. Anthropomorphic Perspex head and neck phantom during IMRT treatment.

images were marked at each Perspex slab as a guidance for assembling the phantom. Twelve (12) OARs were selected including; eyes (bilateral), parotid glands (bilateral), optic nerve (bilateral), temporo-mandibular joint (bilateral), brain stem, optic chiasm, larynx, and spinal cord in addition to both sides of the PTVs including the borderline. One hundred and eleven (111) holes with dimensions of 0.15 cm (diameter) and 0.8 cm (depth) were drilled into various locations within OARs and PTV regions in each slab for placement of TLDs. To avoid any influence on TLDs dose due to the slightly higher density of the TLDs (2.64 g.cm^{-3}) (Santvoort and Heijmen, 1996), holes were drilled at least 1 cm apart. A CT scan was performed to the fabricated phantom to check if the positions of TLDs were within the delineated organs and PTVs.

Phantom planning and reproducibility test

The phantom was planned using nasopharyngeal cancer IMRT treatment plan as follows: Gross disease PTV 70 Gy and dose fractions up to 33 for 5 days a week (Lee et al., 2009). The imaginary contours were drawn for Gross Tumor Volume (GTV), a margin of ≥ 5 mm was given circumferentially around the GTV to draw Clinical Target Volume CTV 70.

A separate PTV provided a margin around the CTV's to compensate the variability of treatment set up and internal organ motion, a minimum of 5 mm around the CTV's was required in all directions to define each respective PTV (PTV 70, PTV 63, PTV 56). These were

delineated on each slab by the treating radiation oncologist. Nine-field (9) IMRT with 6 MV beam energy were used to shoot the phantom three times after loading with TLDs (Figure 4).

Based on reproducibility results of TLDs calibration, a hundred and eleven (111) TLDs were chosen for this study. The TLDs were placed into various locations of interest and were then read, subtracted from background, and then corrected after each treatment.

Phantom implementation for patient's treatment plans verification

Four (4) head and neck patients' treatment plans were chosen and applied on the fabricated phantom by matching the isocenter using TPS. The delineation of OARs and PTVs were then adjusted to ensure that TLDs holes were located within OAR and PTV boundaries. All TLDs dosimeters were read, corrected, and the averages of TLD readings at each region were considered.

Calculated doses were obtained from TPS and compared point-to-point to measured ones and organ-to-organ with the constraints doses according to RTOG 0615 (Lee et al., 2009).

RESULTS AND DISCUSSION

TLDs were calibrated at reference setting using 6 MV photon beam energy. The TLD readings displayed a linear response ($R^2=0.998$) with respect to the measured

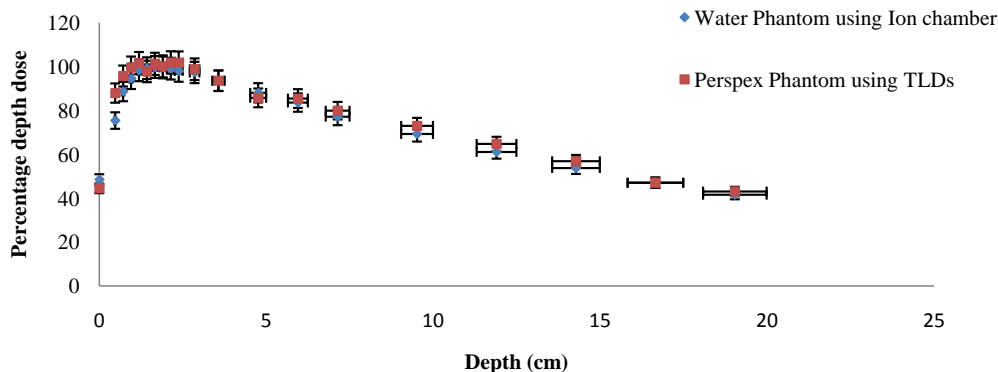


Figure 5. Central axis depth dose distribution for 6 MV photon beam at field size (10 × 10 cm²), SSD=100 cm, using ion chamber in Solid Water Phantom and TLDs in Perspex phantom.

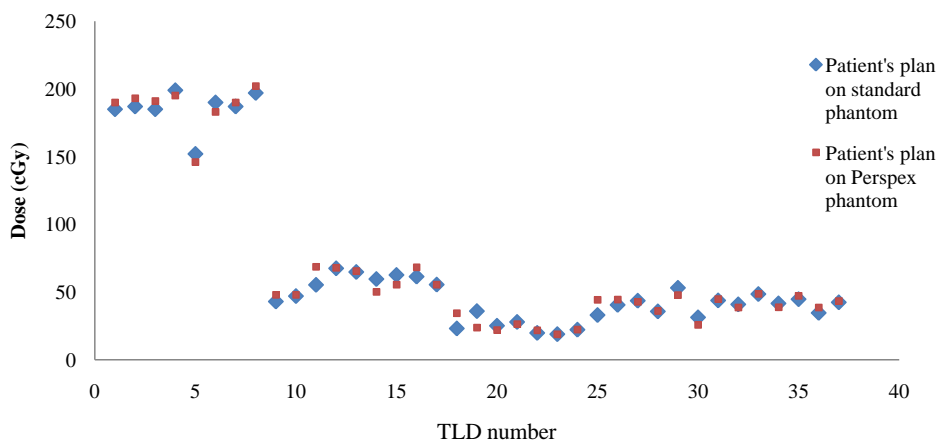


Figure 6. Measured doses (cGy) in cubic Perspex phantom and Scanditronix Wellhöver phantom using IMRT treatment plan.

doses at d_{max} from 50 to 400 cGy. The main reproducibility of the TLDs was within 3% and the sensitivity of 10% at one standard deviation. An energy correction factor of 1.04 for TLD-100 measurement was performed in the outfield where the scattered photons had lower energy than the main energy (Kry et al., 2006). In another study, the energy response of TLD-100 to photons with energy ranging from 200 keV to 3 MeV remained constant and the correction factors were between 4 and 5% (Charalambous and Petridou, 1976). In this study, no energy correction factors were used as the reproducibility of TLD readings had a standard deviation of 3%.

Central axis depth dose distribution for 6 MV photon beam, 10 × 10 cm² field size and 100 cm SSD, using calibrated ion chamber in water phantom and TLDs in Perspex phantom are presented in Figure 5. The mean difference between the two phantoms measured values

was 2.9% with a standard deviation of 4.8%, with the largest difference at the build-up regions. Discrepancies for all depths between d_{max} and 20 cm remained within 2.1% and a standard deviation of 2.6%. In previous literature, correction factors of 1.068 using TLDs and 1.063 using Monte Carlo simulation were found (Lee et al., 2008) and in agreement, it is 1.064 in this study. This correction replaces all corrections for sensitivity, phantom material, field size, and fading.

Since phantom material can be a source of error during dosimetric measurements, attention was paid to find the effect of Perspex material. A cubic Perspex phantom was designed and three CT reference points and isocenter were used to match three chosen points with IMRT phantom (Scanditronix Wellhöver). Both phantoms' results were comparable and the difference between point-to-point doses remained within the acceptable limit of 2% ($P > 0.05$). Figure 6 summarizes the TLD's

Table 1. The average of three delivered doses at different OAR regions using phantom's plan in comparison with radiation therapy oncology group protocol (RTOG 0615).

Organ at risk	# TLDs	Dose constraints (Gy)	The average of three shoots			
			M _{av} ±SD (cG)	M _{av} (Gy)	TPS (cGy)	% Dose difference
Optic chiasm	3	< 54	82.1 ± 3.1	27.1	93.1	11.8
R eye	4	< 45	30.1 ± 2.3	9.9	29.3	2.7
L eye	4	< 45	26.8 ± 2.5	8.9	29.3	8.3
R optic nerve	2	< 54	115.0 ± 5.5	38.0	105.2	9.3
L optic nerve	2	< 54	127.8 ± 5.5	42.2	136.1	6.1
L parotid	4	< 26	61.4 ± 2.0	20.3	57.5	6.8
R parotid	4	< 26	82.0 ± 3.7	27.1	87.3	6.1
R TMJ	2	< 70	115.2 ± 4.4	38.0	104.2	10.6
L TMJ	2	< 70	125.0 ± 4.1	41.3	132.5	5.7
Brainstem	4	< 54	106.2 ± 3.2	35.0	116.6	9.0
Larynx	16	< 45	114.1 ± 6.0	37.6	126.8	10.1
Spinal cord	13	< 45	169.6 ± 4.8	56.0	188.3	10.0
PTV 70	19	> = 70	205.5 ± 5.3	67.8	193.4	6.3
PTV63	18	> = 63	180.0 ± 3.0	59.4	170.4	5.6
PTV 56	10	> = 56	160.0 ± 6.5	52.8	171.2	6.5
Mean						7.7
SD%						2.4

Abbreviations: M_{av} (Gy): Average measurement doses in Gy using TLD, TPS (Gy): Calculated doses using treatment planning system, R: Right, L: Left, TMJ= Temporo-Mandibular Joint.

measurements in both phantoms using the same treatment plan.

To determine how well the phantom's results could be reproduced, treatment plan for the phantom was delivered three times identically. The average point-by-point percent three standard deviation between the three TLD readings at identical settings was less than 3.5%. Furthermore, the average of dose discrepancies between the average of the three TLD readings and TPS were found to be 6.14% at PTVs and 8.0% at OAR with a mean correlation of 0.985 (Table 1).

Verification of IMRT patient's treatment plans was implemented using the study phantom and all delivered doses at OAR and PTV regions were measured and compared with both TPS doses and the constraint doses as recorded by RTOG (Lee et al., 2009). The results were expressed by both; the mean of percent dose differences between measured and TPS calculated doses and the standard deviation of TLD/TPS ratio. The percentage doses differences were found within a range of 5.15 to 7.2% at OARs and 5.13 to 6.6% at PTVs (Table 2). Woo et al. (2003) used a silver halide film in a cubic phantom to verify treatment plan before patient treatment. The maximum dose measured on the film was within 5% of that predicted doses by the planning

computer (Woo et al., 2003). In another study, Low et al. (1998) found the percent dose difference 4% for PTVs and 5% for OARs. Verification of IMRT patient's treatment plans was implemented using the study phantom and all delivered doses at OAR and PTV regions were measured and compared with both TPS doses and the constraint doses as recorded by RTOG (Lee et al., 2009). The results were expressed by both; the mean of percent dose differences between measured and TPS calculated doses and the standard deviation of TLD/TPS ratio. The percentage doses differences were found within a range of 5.15 to 7.2% at OAR and 5.13 to 6.6% at PTVs (Table 2).

There was a good agreement between the doses measured by TLD and those calculated by TPS at the PTVs, with average standard deviation of TLD/TPS ratio being 2.4%. The dose agreement in the OAR was not as close, with an average TLD/TPS ratio of 0.98 and a standard deviation of 6.8% (Table 3). These results showed that the deviation between planned and measured doses have met the accuracy criteria of ± 7% for the primary and secondary PTVs (Molineu et al., 2005; Ibbott et al., 2006).

In Molineu et al. (2005) study, an anthropomorphic head and neck phantom was designed and sent to multi-

Table 2. Dosimetric verification of four (4) nasopharyngeal patients' IMRT treatment plans using the fabricated head and neck phantom.

Organ at risk	# TLD	Dose constraints	Plan 1			Plan 2			Plan 3			Plan 4		
			M _{av} (Gy)	TPS (Gy)	%Dose difference	M _{av} (Gy)	TPS (Gy)	%Dose difference	M _{av} (Gy)	TPS (Gy)	%Dose difference	M _{av} (Gy)	TPS (Gy)	%Dose difference
Optic chiasm	3	< 54 Gy	17.2	16.5	4.2	27.0	28.7	5.9	25.3	26.1	3.1	25.8	24.3	6.2
R eye	4	< 45 Gy	9.8	10.3	4.9	10.2	10.9	6.4	10.9	11.3	3.5	14.6	17.1	14.6
L eye	4	< 45 Gy	6.3	6.9	8.7	7.0	7.1	1.4	7.6	8.1	6.2	9.1	11.2	18.8
R optic nerve	2	< 54 Gy	47.5	49.5	4.0	48.7	50.4	3.4	50.8	51.3	1.0	50.6	53.3	5.1
L optic nerve	2	< 54 Gy	43.6	42.6	2.3	43.0	42.2	1.9	43.5	40.2	8.2	42.5	46.3	8.2
L parotid	4	< 26 Gy	18.1	17.4	4.0	18.2	18.1	0.6	26.8	27.3	1.8	18.5	17.9	3.4
R parotid	4	< 26 Gy	20.3	19.2	5.7	21.2	22.1	4.1	23.1	25.2	8.3	24.3	22.4	8.5
R TMJ	2	< 70 Gy	35.6	38.9	8.5	37.6	43.9	14.4	40.2	39.2	2.6	40.2	39.7	1.3
L TMJ	2	< 70 Gy	22.7	20.7	9.7	23.1	21.2	9.0	26.8	30.1	11.0	23.9	24.3	1.6
Brainstem	4	< 54 Gy	25.4	33.9	25.1	22.4	23.6	5.1	27	25.9	4.2	27.0	25.9	4.2
Larynx	16	< 45 Gy	39.5	38.1	3.7	39.9	37.7	5.8	36.9	42.2	12.6	37.6	38.8	3.1
Spinal cord	13	< 45 Gy	28.4	30.1	5.6	34.1	35.5	3.9	35.8	37.6	4.8	35.1	33.9	3.5
PTV 70	9	> = 70 Gy	62.8	68.5	8.3	62.4	66.7	6.4	63.2	66.9	5.5	62.3	66.9	6.9
PTV63	30	> = 63 Gy	58.4	61.8	5.5	55.1	61.3	10.1	56.6	61.5	8.0	57.4	61.8	7.1
PTV 56	12	> = 56 Gy	55.6	57.4	3.1	59.4	57.5	3.3	57.8	58.9	1.9	58.2	55.2	5.4
Mean					6.9			5.4			5.5			6.5
SD%					5.5			3.6			3.5			4.7

Abbreviations: M_{av} (Gy) =Average measurement doses in Gy using TLD; TPS(Gy)=Calculated doses using treatment planning system; R=Right; L=Left, TMJ= Temporo-Mandibular Joint.

institution for dosimetric verification of IMRT dose delivery. Data collected from irradiations at 10 institutions showed that the TLD agreed with institutions' doses to within 5.7% standard deviation in PTV and 15.6% standard deviation in OAR (Molinue et al., 2005). Discrepancies between the planned and delivered doses especially at OAR may arise because the contribution of out-of-field doses to clinically significant areas which is much higher for IMRT

than for conventional radiotherapy.

Furthermore, there was a small air gap between phantoms' slabs, which could not be completely eliminated.

This mainly developed from the differences in size between the holes that were made slightly bigger than TLDs, in order to avoid TLD's scratching or breaking when assembling the model.

These air gaps could result in increased

exposure to the TLDs due to the decreased amount of attenuation present and may have led to such dose discrepancies.

Conclusion

This is a new handmade design of anthropomorphic head and neck phantom intended for dosimetric verification of IMRT plans.

Table 3. Ratio of the TLD to treatment planning system doses for the four patients' treatment plans used to irradiate the phantom.

Organ at risk	# TLDs	Plan 1	Plan 2	Plan 3	Plan 4	Average	SD%
		TLDs/TPS	TLDs/TPS	TLDs/TPS	TLDs/TPS		
Optic chiasm	3	1.04	0.94	0.97	1.06	1.00	5.8
R eye	4	0.95	0.94	0.96	0.85	0.93	5.0
L eye	4	0.91	0.99	0.94	0.81	0.91	7.3
R optic nerve	2	0.96	0.97	0.99	0.95	0.97	1.7
L optic nerve	2	1.02	1.02	1.08	0.92	1.01	6.8
L parotid	4	1.04	1.01	0.98	1.03	1.02	2.7
R parotid	4	1.06	0.96	0.92	1.08	1.01	8.0
R TMJ	2	0.92	0.86	1.03	1.01	0.96	8.1
L TMJ	2	1.10	1.09	0.89	0.98	1.02	9.8
Brainstem	4	0.75	0.95	1.04	1.04	0.95	13.8
Larynx	16	1.04	1.06	0.87	0.97	0.99	8.3
Spinal cord	13	0.94	0.96	0.95	1.04	0.97	4.2
Average at OARs						0.98	6.8
PTV 70	9	0.92	0.94	0.94	0.93	0.93	1.2
PTV63	30	0.94	0.90	0.92	0.93	0.92	1.9
PTV 56	12	0.97	1.03	0.98	1.05	1.01	4.1
Average at PTVs						0.95	2.4

It was designed with movable slabs, each with delineated clinical organs used to predict delivered doses at any organ of interest. It is possible to make absolute measurement of doses at various depths with a hundred and one (111) positions throughout the phantom with TLDs as well as relative doses by comparing TLDs or film measurements to TPS.

Furthermore, other dosimeters can be used, such as radiochromic film. Point dose measurements in any position in the phantom can be easily measured using MOSFET diodes or TLDs as point dose measurements are critical when evaluating doses to sensitive structures. The anthropomorphic design provided intuitive and easy set-up for fast confirmation of treatment plan. It can interface with treatment planning systems as the TPS recognized the phantom fiducial system and anthropomorphic shape. The TLD measurements were reproducible and able to provide accurate determination of the absolute delivered doses throughout target volumes and critical structures.

The results have preliminary proved that the phantom is a valuable tool in pre-treatment verification program of clinical head and neck treatment plan. It can be used to audit the entire patient pathway for simple head and neck treatments from computed tomography scan through TPS to delivery allowing for verification of absolute dose in regions of clinical and dosimetric interests. Further modifications as finishing and holding techniques will be

considered in future work.

ACKNOWLEDGMENT

This paper is a part of the research done within the project (FRGS), number 203 / PFIZIK / 6711178, Universiti Sains Malaysia (USM), Malaysia. The authors would like to thank all radiologist, physicists and radiographers in the Radiotherapy Department of Mount Miriam Cancer Center in Penang, Malaysia for their cooperation and help.

REFERENCES

- Attix FH (1986). Introduction To Radiological Physics And Radiation Dosimetry, First Ed. Wiley-VCH.
- Cadman P, Bassalow R, Sidhu NPS (2002). Dosimetric considerations for validation of a sequential IMRT process with a commercial treatment planning system. *Phys. Med. Biol.*, 47: 3001–3010.
- Charalambous, S, Petridou C (1976). The thermoluminescence behaviour of LiF (TLD-100) for doses up to 10 MRad. *Nucl. Instrum. Method.*, 137(3): 441-444.
- Chung H, Jin H, Dempsey JF, Liu C, Palta J, Suh TS, Kim S (2005). Evaluation of surface and build-up region

- dose for intensity-modulated radiation therapy in head and neck cancer. *Med. Phys.*, 32: 2682.
- Ezzell GA, Galvin JM, Low D, Palta JR, Rosen I, Sharpe MB (2003). Guidance document on delivery, treatment planning, and clinical implementation of IMRT: Report of the IMRT subcommittee of the AAPM radiation therapy committee. *Med. Phys.*, 30: 2089.
- Furetta C, Weng PS (1998). *Operational Thermoluminescence Dosimetry*, World Scientific Pub Co Inc.
- Galvin JM, Ezzell G, Eisbrauch A, Yu C, Butler B, Xiao Y, Rosen I, Rosenman J, Sharpe M, Xing L, Xia P, Lomax T, Low DA, Palta J (2004). Implementing IMRT in clinical practice: a joint document of the American Society for Therapeutic Radiology and Oncology and the American Association of Physicists in Medicine. *Int. J. Radiat. Oncol. Biol. Phys.*, 58(5): 1616.
- Gillis S, De Wagter C, Bohsung J, Perrin B, Williams P, Mijnheer BJ (2005). An inter-centre quality assurance network for IMRT verification: results of the ESTRO QUASIMODO project. *Radiother. Oncol.*, 76(3): 340-353.
- Horowitz YS (1984). *Thermoluminescence and Thermoluminescent Dosimetry*, First Ed, CRC Press.
- Ibbott GS, Molineu A, Followill DS (2006). Independent evaluations of IMRT through the use of an anthropomorphic phantom. *Technol Cancer Res. T.* 5: 481-487.
- ICRU (International Commission On Radiation Units And Measurements) (1989). *Tissue Substitutes in Radiation Dosimetry and Measurement*. Rep. 44, ICRU, Bethesda, MD
- Kam MKM, Chau R, Suen J, Choi PHK, Teo PML (2003). Intensity-modulated radiotherapy in nasopharyngeal carcinoma: dosimetric advantage over conventional plans and feasibility of dose escalation. *Int. J. Radiat. Oncol. Biol. Phys.*, 56(1): 145-157.
- Kinhikar R, Upreti R, Sharma S, Tambe C, Deshpande D (2007). Intensity modulated radiotherapy dosimetry with ion chambers, TLD, MOSFET and EDR2 film. *Australas Phys. Eng. Sci. Med.*, 30(1): 25-32.
- Kry SF, Titt U, Pönisch F, Followill D, Vassiliev ON, White RA (2006). A Monte Carlo model for calculating out-of-field dose from a Varian 6 MV beam. *Med. Phys.*, 33: 4405.
- Lee J, Yehc C, Hsud S, Shia M, Chend WL, Wangb C (2008). Simple dose verification system for radiotherapy radiation. *Radiat. Measure.*, 43: 954 - 958.
- Lee N, Pfister D, Garden A (2009). RTOG 0615, A phase II study of concurrent chemoradiotherapy using three-dimensional conformal radiotherapy (3D-CRT) or intensity-modulated radiation therapy (IMRT)+ bevacizumab (BV) for locally or regionally advanced nasopharyngeal cancer.
- Low DA, Chao KS, Mutic S, Gerber RL, Perez CA, Purdy JA (1998). Quality assurance of serial tomotherapy for head and neck patient treatments. *Int. J. Radiat. Oncol. Biol. Phys.*, 42(3): 681-692.
- McKeever SWS, Moscovitch M, Townsend P (1995). *Thermoluminescence Dosimetry Materials: Properties And Uses*. Nuclear Technology Publishing.
- Molineu A, Followill DS, Balter PA, Hanson WF, Gillin MT, Huq MS, Eisbruch A, Ibbott GS (2005). Design and implementation of an anthropomorphic quality assurance phantom, for intensity-modulated radiation therapy for the Radiation Therapy Oncology Group. *Int. J. Radiat. Oncol. Biol. Phys.*, 63: 577-583.
- Radaideh KM, Alzoubi AS (2010). Factors impacting the dose at maximum depth dose (d_{max}) for 6 MV high-energy photon beams using different dosimetric detectors. *Bioheal. Sci. Bull.*, 2(2): 38-42.
- Santvoort JPC, Heijmen B (1996). Dynamic multileaf collimation without tongue-and-groove underdosage effects. *Phys. Med. Biol.*, 41: 2091.
- Van Esch A, Bohsung J, Sorvari P, Tenhunen M, Pausco M, Iori M (2002). Acceptance tests and quality control (QC) procedures for the clinical implementation of intensity modulated radiotherapy (IMRT) using inverse planning and the sliding window technique: experience from five radiotherapy departments. *Radiother. Oncol.* 65(1): 53-70.
- Webster GJ (2008). Design and implementation of a head & neck phantom (HANK) for system audit and verification of IMRT. *J. Appl. Clin. Med. Phys.*, 9(2).
- Woo SY, Grant W 3rd, McGary JE, Teh BS, Butler EB (2003). The evolution of quality assurance for intensity-modulated radiation therapy (IMRT): Sequential Tomotherapy, 56(1):274-286.
- Yazici N (2004). The influence of heating rate on the TL response of the main glow peaks 5 and 4+ 5 of sensitized TLD-100 treated by two different annealing protocols. *Nucl. Instrum. Method.*, 215(1-2): 174-180.